Poly[*N*-(2-hydroxypropyl)methacrylamide] Polymers Diffuse in Brain Extracellular Space with Same Tortuosity as Small Molecules

Š. Prokopová-Kubinová,* L. Vargová,* L. Tao,† K. Ulbrich,‡ V. Šubr,‡ E. Syková,* and C. Nicholson†

*Department of Neuroscience, Second Faculty of Medicine, Charles University, and Institute of Experimental Medicine, Academy of Sciences of the Czech Republic, 142 20 Prague, Czech Republic; †Department of Physiology and Neuroscience, New York University School of Medicine, New York, New York 10016 USA; and ‡Institute of Macromolecular Chemistry, Academy of Sciences of the Czech Republic, 162 06 Prague, Czech Republic

ABSTRACT Integrative optical imaging was used to show that long-chain synthetic poly[*N*-(2-hydroxypropyl)methacrylamide] (PHPMA) polymers in a range of molecular weights from 7.8 to 1057 kDa were able to diffuse through the extracellular space in rat neocortical slices. Tortuosity (square root of ratio of diffusion coefficient in aqueous medium to that in brain) measured with such polymers averaged 1.57, a value similar to that obtained previously with tetramethylammonium, a small cation. When PHPMA was conjugated with bovine serum albumin (BSA) to make a bulky polymer with molecular weight 176 kDa, the tortuosity rose to 2.27, a value similar to that obtained previously with BSA alone and with 70-kDa dextran. The method of image analysis was justified with diffusion models involving spherical and nonspherical initial distributions of the molecules.

INTRODUCTION

From a physical perspective, the extracellular space (ECS) of the brain is a porous medium. In the neuroscience context, the ECS is a conduit for cellular metabolites, a channel for chemical signaling mediated by volume transmission, and a route for drug delivery. The ECS occupies ~20% of brain volume, i.e., the extracellular volume fraction α is ~0.2 (Nicholson and Syková, 1998), but interstitial spaces are narrow and small molecules (~100 M_r) undergo hindered diffusion, described by a tortuosity factor λ of ~1.6, where $\lambda = (D/D^*)^{1/2}$ and D and D^* are the diffusion coefficients in free medium and in brain tissue, respectively (Nicholson and Phillips, 1981; Nicholson and Syková, 1998).

Macromolecules, such as dextran (70-kDa M_r) and bovine serum albumin (BSA; 66-kDa M_r), also diffuse in the ECS but with a tortuosity of ~2.3, suggesting that their larger size and globular shape cause more obstruction (Nicholson and Tao, 1993; Tao, 1999; Tao and Nicholson, 1996). Molecules of poly[*N*-(2-hydroxypropyl)methacrylamide] (PHPMA) are synthetic, linear, water-soluble polymers that are being developed for drug delivery. The polymers consist of repeating subunits with an occasional spacer to attach a drug molecule or other moiety (Ulbrich et al., 1997). Here we show that PHPMA polymers as large as 1057-kDa M_r can move through the brain with the same λ-value as a small molecule. When, however, a bulky PHPMA-BSA branched polymer was used, the tortuosity increased to ~2.3. These results indicate that some large linear macromolecules are able to diffuse through the ECS while experiencing only the same hindrance as do small molecules.

Received for publication 12 July 2000 and in final form 5 October 2000.

Address reprint requests to Dr. Charles Nicholson, Department of Physiology and Neuroscience, NYU School of Medicine, 550 First Avenue, New York, NY 10016. Tel.: 212-263-5421; Fax: 212-689-9060; E-mail: charles.nicholson@nyu.edu.

0006-3495/01/01/542/07 $2.00

MATERIALS AND METHODS

PHPMA polymers

Narrow fractions of linear, water-soluble PHPMA polymers with M_r values 7.8, 28.0, 47.2, 220, 515, and 1057 were prepared by radical polymerization followed by gel permeation chromatography GPC fractionation (Noguchi et al., 1998; Šubr et al. 1997). To enable the diffusion of the polymers to be imaged, a fluorescent marker (FITC or Texas Red) was attached to the PHPMA. Polymers of PHPMA also can be conjugated with proteins to form high-molecular-weight branched conjugates; in this study BSA was modified by attaching PHPMA polymers bearing covalently bonded FITC. This conjugate had an M_r of 176 kDa and consisted of 25 wt % BSA and 75 wt % synthetic polymer of 23-kDa M_r. The final result was a branched or bulky polymer structure with the BSA at the center and several chains of PHPMA attached.

Cortical slice preparation

The slice preparation has been described in detail (Nicholson and Tao, 1993; Pérez-Pinzón et al., 1995; Rice and Nicholson, 1991). Female Sprague Dawley rats (150–250 g) were deeply anesthetized with sodium pentobarbital (65 mg kg^{-1}) and decapitated, and the brains were removed. Tissue was sectioned with a Camden Vibroslice (WPI, Sarasota, FL) at a thickness of 400 μm and stored in artificial cerebrospinal fluid (ACSF) at room temperature for ~1 h before use. The ACSF contained (in mM): 124 NaCl, 26 $NaHCO_3$, 5 KCl, 1.25 NaH_2PO_4, 1.5 $CaCl_2$, 1.3 $MgCl_2$, 10 glucose. The ACSF was gassed with 95% O_2/5% CO_2 (to buffer pH at 7.4, in conjunction with the HCO_3).

Slices were held in a submersion chamber (type RC-27L or RC-29, Warner Instrument Corp., Hamden, CT) mounted in the center of a fixed stage (Gibralter; Burleigh Instruments, Fishers, NY) under a compound microscope (BW50WI, Olympus Optical Co., Tokyo, Japan). Oxygenated ACSF was pumped at a rate of ~1.5 ml min^{-1} with a peristaltic pump, and all experiments were performed at 34°C. Characteristic field potentials (Rosen and Andrew, 1990), evoked by local stimulation and recorded with a microelectrode, were used to assess slice viability in some experiments.

Slices were considered viable if stable field potentials could be recorded for 30–60 min.

Integrative optical imaging (IOI) to determine apparent diffusion coefficient

In the IOI method (Nicholson and Tao, 1993) macromolecules are released from a micropipette by a brief pulse of nitrogen delivered by an electronically controlled valve (General Valve, Fairfield, NJ). Then the diffusion equation, in spherical coordinates, is (Nicholson and Phillips 1981; Nicholson, 1992)

$$\frac{\partial C_p}{\partial t} = \frac{D^*}{r}\frac{\partial^2 (rC_p)}{\partial r^2} + \frac{1000 n_{PHPMA}}{\alpha}\frac{\delta(r)\delta(t)}{r^2} - k' C_p, \qquad (1)$$

where a concentration C_p (mM), at time t (s) and distance r (cm), results from the amount of substance injected, n_{PHPMA} (mmol). The amount $n_{PHPMA} = UC_f$, where a small volume U (L) at concentration C_f (mM) is actually ejected into the tissue, but it is assumed that, although finite in quantity, the ejected substance occupies a vanishingly small volume relative to the volume in which measurements will be made. The point source in space and time can then be represented by the product of two δ-functions. The apparent (or effective) diffusion coefficient in the tissue is D^* ($cm^2\ s^{-1}$). A linear uptake term, $-k'C_p$, has been included (Nicholson, 1992) for generality, where k' (s^{-1}) is the uptake parameter. The solution to Eq. 1 is given by Nicholson (1985, 1992):

$$C_p(r, t) = \frac{1000 n_{PHPMA}}{\alpha(4D^*(t + t_o)\pi)^{3/2}} \exp\left(\frac{-r^2}{4D^*(t + t_o)} - k'(t + t_o)\right) \qquad (2)$$

The term t_o (s) represents a virtual source-time origin such that the source appears to have been activated at a time t_o before it actually occurred. The reason for the inclusion of this term will be explained later. It is assumed that $k' = 0$ for the PHPMA molecules because it is unlikely that such large molecules are able to enter cells over the time span of the measurements and because the data analysis provides good fits of Eq. 2 when $k' = 0$.

In these experiments a sub-nanoliter amount of the fluorescent PHPMA in isotonic saline at a concentration of 0.1–1.0 mM was pressure ejected from a micropipette into the center of the slice with a nitrogen pulse less than 1 s in duration. The diameter of the tip of the micropipette was 2–6 μm, and so it was effectively a point source.

The basic experimental setup has been detailed by Nicholson and Tao (1993). The IOI system used in the present experiments consisted of an Olympus BX50WI microscope with a water-immersion objective (Olympus UM PlanFl 10×, NA 0.3), a 100-W halogen epi-illuminator, and a dichroic mirror system and filters appropriate to the fluorophore in use. The image was recorded by a charge-coupled device (CCD) camera cooled to −40°C (model CH350, Photometrics, Tucson, AZ) equipped with a Thompson CCD array with 576 × 384 pixels and 14-bit resolution. The camera exposure time was 50–400 ms. The output of the camera was transferred directly to a Pentium PC, and images were acquired using the V-Pascal language (Photometrics) to control the camera and computer.

After image acquisition, the diffusion analysis (see below) was performed with the program IDA (written by C. Nicholson, based on a previous program by L. Tao) running under MATLAB (The Math Works, Natick, MA). The theory of how the image of the diffusing cloud of molecules maps onto the plane of the CCD camera is quite complex. Nevertheless, it can be reduced to a basic equation, derived from Eq. 2. The camera images are taken at a sequence of discrete times t_i, and the fluorescence intensity I_i at any radius r in the slice from the point source location, assuming that the molecules diffuse out with spherical symmetry from the origin, is given by

$$I_i(r, \gamma_i) = E_i(\gamma_i) e^{-(r/\gamma_i)^2}, \qquad (3)$$

where E_i is an amplitude term embodying the de-focused point spread function of the objective (Nicholson and Tao, 1993; Tao and Nicholson, 1995). This term is independent of r. The term γ_i is given by

$$\gamma_i^2 = 4D^*(t_i + t_o). \qquad (4)$$

By fitting the exponential term in Eq. 3 to the spatial distribution at each time t_i, D^* can be determined from Eq. 4. In practice, use is made of the redundant information available in the whole sequence of time measurements to further enhance accuracy by using several images corresponding to a sequence of t_i to obtain γ_i and then performing a linear regression according to Eq. 4 to obtain D^* and t_o.

The use of the virtual source-time origin can now be justified. Eqs. 2 and 3 are based on the assumption that molecules start from a point source in both space and time. This is a good approximation in time because the duration of the pressure pulse used to release the molecules is in the range 100-1000 ms whereas the analysis times are typically at intervals of 10–50 s. But the initial distribution of molecules can occupy a volume in the tissue of 20–150-μm diameter. As time progresses, however, the diffusion process erases the detail of the source structure so that it is possible to attribute the diffusing cloud of molecules to a virtual point source that was delivered at time t_o before the actual delivery. This works well in practice, and later in the paper we will justify the process with a simulation based on the results. The actual analytical expression for a finite-volume source will be given later also; this could be used in the fitting procedure but would increase the complexity and does not appear necessary. The even more complex case of a finite, nonspherical initial distribution will also be addressed.

For the reasons just given, no attempt was made to analyze data immediately after the time of ejection, and the first image used was usually taken 10–50 s later.

To determine D, similar measurements were made in 0.3% w/v agarose (NuSieve, FMC Corp. Rockland, ME) dissolved in isotonic saline to give a thin gel. All measurements were made at 34°C. As seen in other studies (Nicholson and Tao, 1993; Tao and Nicholson, 1996), agarose at this concentration does not significantly impede diffusion. This was confirmed here when the data obtained here with IOI were compared to diffusion coefficients obtained with light-scattering measurements made when the PHPMA polymers were synthesized. Diffusion coefficients (measured in units of 10^{-7} $cm^2\ s^{-1}$) obtained for each polymer by light scattering in water at 25°C and corrected to 34°C were as follows: 7.8 kDa, 13.5; 28 kDa, 6.35; 47.2 kDa, 4.55; 220 kDa, 2.16; 515 kDa, 1.08; 1057 kDa, 0.72. Apart from some deviation for the smallest polymer, these values are similar to those obtained subsequently with IOI.

Nonspherical model source

When molecules were pressure-ejected, the initial distribution was often slightly elliptical and the molecules were not centered on the tip of the ejecting electrode, but the center of the distribution was somewhat below the tip. For small molecules (e.g., 7.8-kDa PHPMA) the cloud rapidly became spherical, but for large molecules the asymmetry persisted throughout most of the analysis. To check that this would not produce significant errors, a model was constructed of an extended nonspherical source distribution.

The diffusion was simulated by populating a three-dimensional ellipsoidal volume with $M = 2500$ point sources (Fig. 1) and calculating, by linear summation, the appropriate concentration distribution in the surrounding space from the point-source diffusion equation (Eq. 2) with $t_o = 0$:

$$C(r, t) = \frac{1}{M}\sum_{j=1}^{M} C_p(|\mathbf{r} - \mathbf{r}_j|, t), \qquad (5)$$

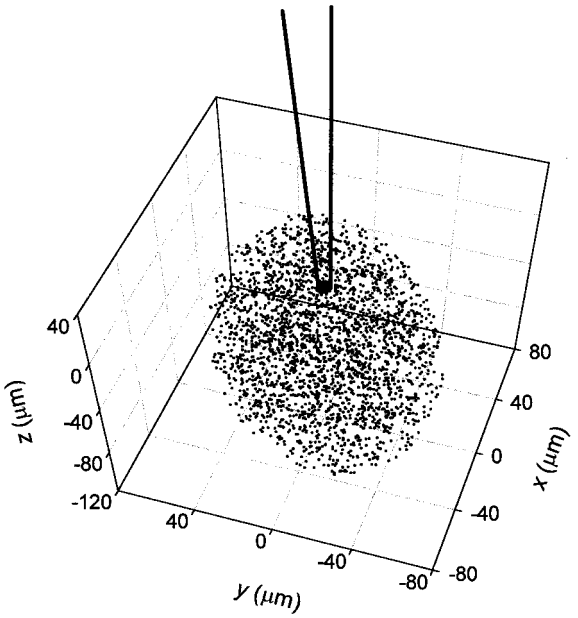

FIGURE 1 Ellipsoidal source distribution. The model consisted of 2500 point sources randomly distributed in an ellipsoidal volume with semi-axes (b_1, b_2, and b_3) of length 81, 54, 54 μm, respectively, for the initial distribution in the ECS, resulting from the injection of 0.2 nl into ECS with a volume fraction of $\alpha = 0.2$. The center of the ellipsoid was located at $z = -45$ μm, below the observing plane, and the major x-y plane of the ellipsoid was rotated by 30° around the vertical. The tip of the schematic microelectrode, used to eject the molecules, was located at (0,0,0). This model was used to calculate the images in Fig. 2 *C*.

where $\mathbf{r} \equiv (x, y, z)$, the observation point, and $\mathbf{r}_j \equiv (x_j, y_j, z_j)$ is the location of the jth source, $r \equiv |\mathbf{r}| \equiv \sqrt{x^2 + y^2 + z^2}$. The distributions in the plane $z = 0$, simulating the image plane, were then analyzed with the program IDA. The semi-major axes of the ellipsoid, b_1, b_2, b_3 (cm), and the volume injected, U (L), are related by $U = 4\pi\alpha b_1 b_2 b_3/3000$, and the amount of substance injected is given by $n_{\mathrm{PHPMA}} = UC_{\mathrm{f}}$.

To further assess the accuracy of results obtained with Eq. 2, as the basis for analysis, some calculations were also done with the analytical solution to Eq. 1 when the amount injected initially fills a finite volume of the ECS. Then the initial radius of injected PHPMA in the tissue is b (cm), and the volume injected from the pipette is U (L), so that $U = 4\pi\alpha b^3/3000$, and again, the amount of substance injected is given by $n_{\mathrm{PHPMA}} = UC_{\mathrm{f}}$ (Nicholson, 1985, 1992):

$$C(r, t) = \frac{C_{\mathrm{f}}}{2}\left[\mathrm{erf}(f_+) - \mathrm{erf}(f_-) + \frac{2}{r}\sqrt{\frac{D^*t}{\pi}}\left[\exp(-f_+^2) - \exp(-f_-^2)\right]\right]\exp(-k't), \quad (6)$$

where $f_+ = (r + b)/2\sqrt{D^*t}$ and $f_- = (r - b)/2\sqrt{D^*t}$. The variable b (cm) is the initial radius of injected PHPMA, assumed to be deposited instantaneously with a concentration C_{f} in the form of a spherical drop. The other variables are as previously defined.

In this model, the neocortex was assumed to be isotropic because detailed diffusion measurements with tetramethylammonium (TMA^+) had confirmed this (Mazel et al., 1998). The IOI method has the potential to measure anisotropy (i.e., different values of D^* associated with different directions), and preliminary work on this topic has been presented (Nicholson et al. 1999).

RESULTS

Measurements were made with PHPMA polymers with M_{r} values 7.8, 28.0, 47.2, 220, 515, and 1057. A sequence of images of 515-kDa M_{r} linear PHPMA labeled with FITC diffusing in brain are shown in Fig. 2 *A*. The images were acquired after a brief injection of the polymer from a micropipette at a depth of ~200 μm below the slice surface (total slice thickness, 400 μm). Each image represents a 180-μm x 180-μm area of the neocortical brain slice at the times indicated after the initial release of the fluorescent molecules. The amplitude, shown in false color (red highest, blue lowest), represents the fluorescent intensity, which is proportional to the concentration of the polymer. The typical bell-shaped distributions of intensity shown in Fig. 2 *B*, corresponding to polymer concentration, were measured along a horizontal axis running through the center of each image. The blue lines are the data and the magenta lines are the diffusion curves, fitted using the program IDA and Eq. 3. From these curves γ^2 was determined using Eq. 4 and hence the apparent diffusion coefficient D^*, resulting in a value of 0.38×10^{-7} cm^2 s^{-1} (at 34°C) for this set of images. The curves show the collapse and broadening, characteristic of diffusing molecules, despite the high molecular weight and the fact that the diffusion is taking place in the ECS of brain tissue.

To confirm that the behavior of the images was consistent with basic diffusion theory, a sequence of images (Fig. 2 *C*) was generated using the nonspherical source model (Fig. 1; Eq. 5) to simulate the experiment depicted in Fig. 2 *A*. The shape and location of the source distribution were chosen to give a good fit to the experimental images. A value of 0.39×10^{-7} cm^2 s^{-1} was used for D^* in the model. The value of D^* extracted from the curve fitting to the images generated from the model data (Fig. 2 *D*) was 0.38×10^{-7} cm^2 s^{-1}.

The slight broadening of the experimental images and curves in Fig. 2, *A* and *B,* can be attributed to a small amount of light scatter in the tissue, which was not present in the model. This did not appreciably affect the extraction of D^* from the data.

The values of D and D^* obtained in all the experiments using linear PHPMA molecules are shown on a log-log plot in Fig. 3 and in Table 1. It is evident that the diffusion coefficients in both free medium and brain conformed to a power law relation of the form $D = a\,(M_{\mathrm{r}})^{\mathrm{d}}$. For the dilute agarose $a = 14.6 \times 10^{-5}$ and $d = -0.54$ ($r^2 = 0.99$), whereas for the brain tissue $a = 5.25 \times 10^{-5}$ and $d = -0.53$ ($r^2 = 0.99$). Thus D and D^* vary almost as $(M_{\mathrm{r}})^{-0.5}$, a relation characteristic of molecules of <1000 M_{r} rather than the $d = -0.33$ exponent characteristic of large ones (Rubinow, 1975). Averaging the individual values of λ for the linear-chain PHPMA molecules in the range 7.8–1057 kDa (Table 1) gave $\lambda = 1.57$.

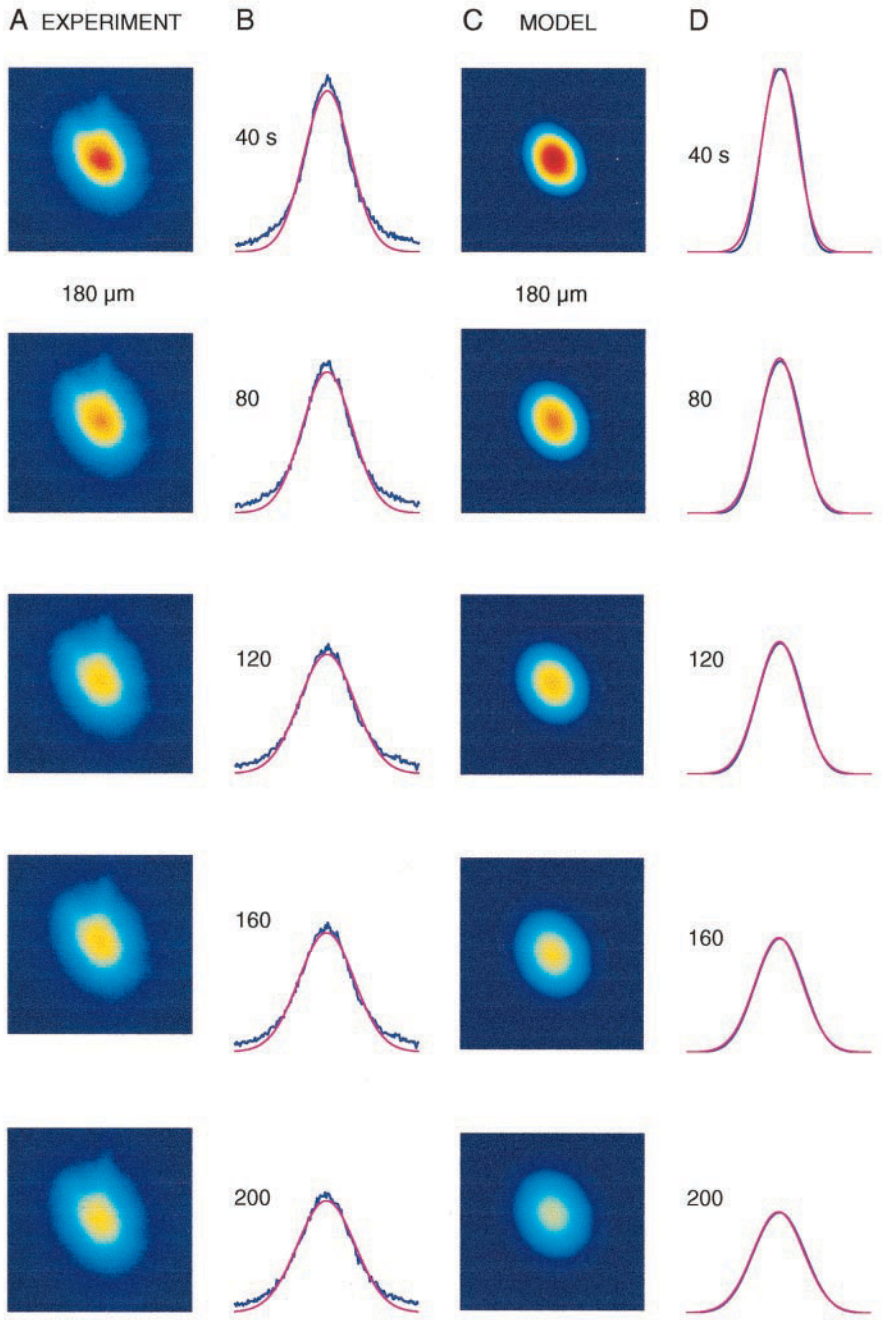

FIGURE 2 Sequence of images and diffusion analysis of 515-kDa M_r linear-PHPMA labeled with FITC diffusing in brain. (*A*) Each image represents a 180-μm x 180-μm area of the neocortical brain slice, as recorded from above using a CCD camera and a compound microscope with a 10× water-immersion objective at the times indicated after the initial release of the fluorescent molecules. The amplitude, shown in false color (red highest, blue lowest), represents the fluorescent intensity, which is proportional to the concentration of the polymer. The initial concentration was established by a brief injection of the polymer from a micropipette at a depth of ~200 μm below the slice surface (total slice thickness, 400 μm). (*B*) The typical bell-shaped distributions of intensity, corresponding to polymer concentration, were measured along a horizontal axis running through the center of each image. The blue lines are the data, and the magenta lines are the diffusion curves, fitted by the analysis program, from which the apparent diffusion coefficient D^* was measured (Nicholson and Tao, 1993) resulting in a value of 0.38×10^{-7} cm^2 s^{-1} for this set of images (34°C). (*C*) Sequence of images produced by the source model shown in Fig. 1 simulating the experiment depicted in *A* to verify the analysis. (*D*) Intensity curves derived from images in *C*. A value of 0.39×10^{-7} cm^2 s^{-1} was used for D^* in the model, and the value of D^* extracted from the curve fitting to the model data was 0.38×10^{-7} cm^2 s^{-1}. The slight broadening of the images and curves in *A* and *B* can be attributed to a small amount of light scatter in the tissue, which is not present in the model shown in *C* and *D*. This does not appreciably affect the extraction of D^* from the data.

In contrast to these results using PHPMA, previous studies using identical experimental methods with two other large molecules, 70-kDa M_r dextran (Nicholson and Tao, 1993) and 66-kDa M_r BSA (Tao and Nicholson, 1996), gave tortuosities of 2.25 and 2.26, respectively (Table 1). Dextran at this molecular weight has a loose spherical shape (Ogston and Woods, 1953) whereas BSA is an ellipsoidal protein (Wright and Thompson, 1975). To determine whether the PHPMA itself was in some way reducing the tortuosity, or whether the effect was related to molecular shape, we used the bulky PHPMA-BSA branched polymer. When diffusion measurements were made with this structure, λ increased to 2.27 (Table 1), which was almost the same value as that obtained with BSA alone.

To appreciate what the experimental values of D^* meant in practical terms, and to verify that the earlier, virtual point source was a good approximation, Fig. 4 shows the concentration versus distance and time profiles for the six PHPMA molecules. In Fig. 4 *A*, the profiles are calculated as a function of distance r for a fixed time $t = 120$ s. The

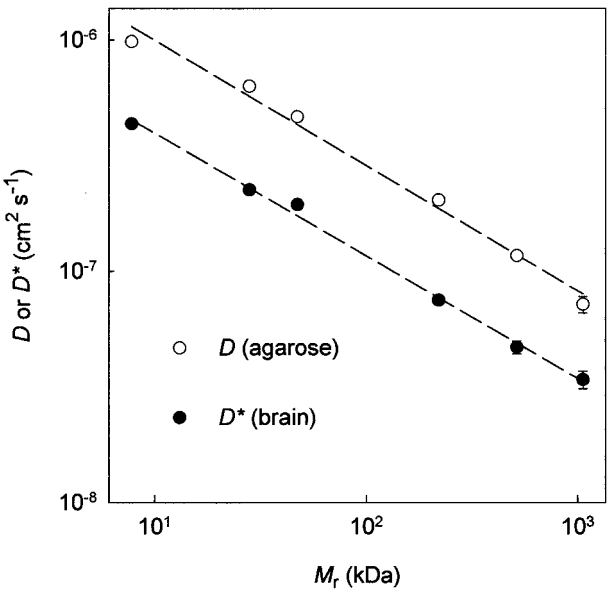

FIGURE 3 Power-law relation between D (agarose) or D^* (brain) and M_r for linear-PHPMA molecules ranging from 7.8-kDa to 1057-kDa M_r. Dashed lines represent linear regressions through the respective data points. Data are taken from Table 1. Further description is in the text.

continuous lines were calculated using the finite volume source equation, Eq. 6, with $U = 0.2$ nl, whereas the dashed lines were calculated from Eq. 2. The virtual point source-time for each molecule was calculated as $t_o = \beta b^2/6D^*$ where β was an arbitrary factor chosen to allow a good fit to the whole family of curves. The factor $b^2/6D^*$ was chosen as providing a suitable characteristic time for a three-dimensional diffusion problem (Nicholson et al., 2000). Because β was the only free parameter, this tested the general validity of the delayed point source concept; here the value $\beta = 0.67$ was used for all curves in Fig. 4, *A* and *B*. In experiments, t_o is extracted by curve fitting. From Fig. 4 *A*, it is evident that, for all the smaller molecules, the virtual point source approximation is very good, and even for the two largest molecules only the peak values near the origin are in error; however, this constitutes a small percentage of the curve. A similar result is evident in Fig. 4 *B* when the curves are plotted as concentrations versus time at a fixed distance of 100 μm from the origin. Here, all the curves with the finite volume and virtual point source are very close, except at very early times. This would be expected, because here the virtual point source approximation would be least accurate; these early times are excluded from the experimental analysis.

Note the interesting result, shown in Fig. 4 *B*, that, because the amount of each molecule ejected is the same ($n_{PHPMA} = 2 \times 10^{-14}$ mol), the peak concentrations at a given distance are also equal and independent of D^* and hence molecular weight. This is a consequence of basic diffusion theory, which indicates that the amplitude is $0.0736\ n_{PHPMA}/(\alpha r^3)$ (Nicholson et al., 2000).

DISCUSSION

Diffusion in the ECS is a process that can be described in both macroscopic and microscopic terms. The macroscopic description is based on solutions of partial differential equations, arising from Fick's Law, whereas the source of the microscopic description is the random walk, arising from Brownian motion. These viewpoints lead to complementary descriptions of diffusion in a porous medium, such as that formed by the intercellular clefts of brain tissue. Here the concept of tortuosity is particularly useful. Formally, tortuosity is a macroscopic parameter based on the ratio of the diffusion coefficient in an unobstructed medium to that in the porous medium. Microscopically, tortuosity is thought of as a measure of the hindrance imposed by the structure of the medium (cells of the brain in the present context) on the molecules as they execute random walks in the void spaces. The link between these two viewpoints is nontrivial and the subject of numerous publications (e.g., Blum et al., 1989;

TABLE 1 Diffusion parameters in 0.3% agarose and brain at 34°C

Molecule	M_r (kDa)	Agarose (D (10^{-7} cm^2 s^{-1}))	Brain slice (D^* (10^{-7} cm^2 s^{-1}))	Tortuosity ($\lambda = (D/D^*)^{1/2}$)
Linear-PHPMA	7.8	9.84 ± 0.21 (36)	4.34 ± 0.12 (28)	1.51 ± 0.04
	28.0	6.30 ± 0.19 (23)	2.25 ± 0.10 (24)	1.67 ± 0.06
	47.2	4.65 ± 0.13 (32)	1.94 ± 0.08 (32)	1.55 ± 0.05
	220	2.03 ± 0.02 (53)	0.75 ± 0.02 (52)	1.65 ± 0.03
	515	1.17 ± 0.05 (31)	0.47 ± 0.03 (29)	1.58 ± 0.08
	1057	0.72 ± 0.06 (25)	0.34 ± 0.03 (29)	1.46 ± 0.12
PHPMA-BSA	175.8	2.34 ± 0.05 (54)	0.45 ± 0.01 (53)	2.27 ± 0.06
Dextran*	70.0	3.80 ± 0.08 (8)	0.75 ± 0.05 (12)	2.25 ± 0.09
Albumin†	66.0	8.29 ± 0.17 (43)	1.63 ± 0.07 (43)	2.26 ± 0.07

Values are mean ± SEM. Number of separate dye ejection experiments is in parentheses. Errors for λ are calculated as $\pm\ 0.5\lambda\ (D_{SEM}/D + D^*_{SEM}/D^*)$, where D_{SEM}, D^*_{SEM} are the standard errors of the means (Nicholson and Tao, 1993).
*Data from Nicholson and Tao (1993).
†Data from Tao and Nicholson (1996).

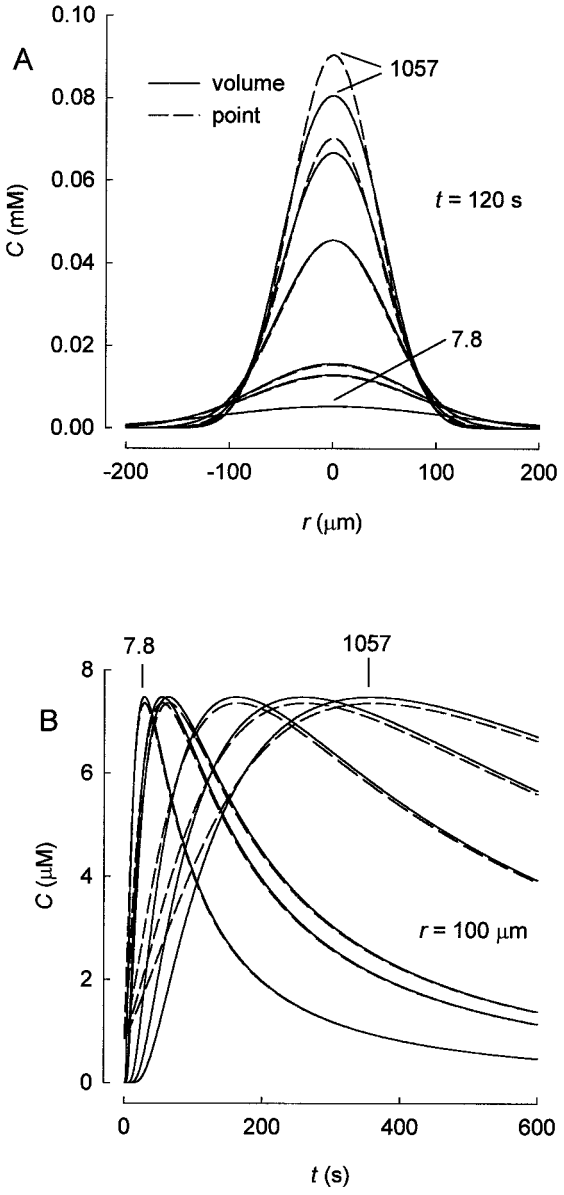

FIGURE 4 Comparison of finite volume source and virtual point source. (*A*) Concentration distribution is calculated as a function of distance at time 120 s after injection of 0.2 nl of PHPMA linear polymers with M_r of 7.8, 28, 47.2, 220, 515, and 1057 kDa using the values of D^* provide in Table 1 and $\alpha = 0.2$. The concentration was 0.1 mM so that the total amount of each polymer released was 20 fmol. For the finite volume source (Eq. 6) this amount infiltrated the ECS and occupied a spherical volume with a radius $b = 62$ μm. The solid lines represented the distribution with this source. The dashed lines show curves derived from using a virtual point source activated at a time t_o before actual delivery, using Eq. 2. The value of t_o was established from the relation $t_o = \beta b^2/6D^*$ where β was an arbitrary factor (here 0.67) chosen to allow a good fit to most of curves. The values of t_o were 10.2, 19.7, 22.8, 59.0, 94.2, and 130.2 s, corresponding to the six PHPMA molecules in the sequence from 7.8 to 1057 kDa, respectively. (*B*) Concentration curves as a function of time at a fixed distance of 100 μm from the source. The same parameters were used as in *A*. This figure shows that both the finite volume and virtual point source gave similar curves (except at early times) and that the amplitude for a fixed distance is independent of the value of D^* (and hence independent of molecular weight) for the same amount of substance (n_{PHPMA}).

Chen and Nicholson, 2000; El-Kareh et al., 1993; Rusakov and Kullmann, 1998).

Our results suggest that PHPMA linear polymers are able to move through the ECS with no more hindrance than that associated with small molecules, though with much reduced D^*, of course. The value of λ obtained here is essentially the same as has been obtained in many studies with the small cation TMA^+ ($M_r = 74$), using a different method for determining D, D^*, and tortuosity (Nicholson and Phillips, 1981). The extensive TMA^+ data are summarized in recent reviews (Syková, 1997; Nicholson and Syková, 1998) and indicate that the minimum value of λ obtained with the small molecule is 1.5–1.7 in many brain regions under normal conditions. In some areas, anisotropy must be taken into account (Rice et al., 1993; Mazel et al., 1998).

A recent paper by Pluen et al. (1999) showed that D^* for long polymers of DNA diffusing in free solution or 2% agarose obeys almost the same power law (exponent -0.52) as a function of the number of base pairs as we have shown here (exponent -0.53) for long-chain PHPMA molecules as a function of molecular weight. Above 6000 base pairs, however, the exponent measured by Pluen et al. suddenly increases sharply, which the authors attributed to reptation (de Gennes 1975). Our data suggest that linear PHPMA polymers, even up to 1000 kDa, are able to diffuse normally in the ECS, and it is globular molecules that are obstructed; Pluen et al. reached a similar conclusion in their studies on relatively dense agarose.

The significance of the fact that the same small value of λ is obtained with linear synthetic PHPMA chains in brain tissue, and presumably other molecules with this type of structure, is that they should be no more hindered than a small molecule in the ECS. This will be important for the transmission of molecular signals in the ECS by volume transmission (Fuxe and Agnati, 1991; Zoli et al., 1999; Agnati et al., 2000) and for drug delivery (Haller and Saltzman, 1998). By the same argument, the data presented here for other classes of large molecules, with a more compact structure, suggest that they could be excluded from certain sites. Such exclusion may be subject to dynamic control as the ECS varies in size (Tao, 1999). These results will be relevant when PHPMA polymers are used to deliver drugs to brain tumors.

This work was supported by National Institutes of Health grant NS 28642 from NINDS (C.N.) and grants GACR 307/96/K226 (K.U. and E.S.) and GACR 309/99/0657 (E.S.)

REFERENCES

Agnati, L. F., K. Fuxe, C. Nicholson, and E. Syková, editors. 2000. Volume Transmission Revisited. Elsevier, Amsterdam.

Blum, J. J., G. Lawler, M. Reed, and I. Shin. 1989. Effect of cytoskeletal geometry on intracellular diffusion. *Biophys. J.* 56:995–1005.

Chen, K. C., and C. Nicholson. 2000. Changes in brain cell shape create residual extracellular space volume and explain tortuosity behavior during osmotic challenge. *Proc. Natl. Acad. Sci. U.S.A.* 97:8306–8311.

de Gennes, P. G. 1975. Scaling Concepts in Polymer Physics. Cornell University Press, Ithaca, NY.

El-Kareh, A. W., S. L. Braunstein, and T. W. Secomb. 1993. Effect of cell arrangement and interstitial volume fraction on the diffusivity of monoclonal antibodies in tissue. *Biophys. J.* 64:1638–1646.

Fuxe, K., and L. F. Agnati (editors). 1991. Volume Transmission in the Brain: Advances in Neuroscience, Vol. 1. Raven Press, New York.

Haller, M. F., and W. M. Saltzman. 1998. Localized delivery of proteins in the brain: can transport be customized? *Pharm. Res.* 15:377–385.

Mazel, T., Z. Šimonová, and E. Syková. 1998. Diffusion heterogeneity and anisotropy in rat hippocampus. *Neuroreport.* 9:1299–1304.

Nicholson, C. 1985. Diffusion from an injected volume of substance in brain tissue with arbitrary volume fraction and tortuosity. *Brain Res.* 333:325–329.

Nicholson, C. 1992. Quantitative analysis of extracellular space using the method of TMA^+ iontophoresis and the issue of TMA^+ uptake. *Can. J. Physiol. Pharmacol.* 70:S314–S322.

Nicholson, C., K. C. Chen, S. Hrabětová, and L. Tao. 2000. Diffusion of molecules in brain extracellular space: theory and experiment. *In* Volume Transmission Revisited. L. F. Agnati, K. Fuxe, C. Nicholson, and E. Syková, editors. Elsevier, Amsterdam. 123–148.

Nicholson, C., S. J. Cragg, and M. E. Rice. 1999. Diffusion anisotropy determined from fluorescent image sequences with application to substantia nigra and VTA. *Soc. Neurosci. Abstr.* 25:743.

Nicholson, C., and J. M. Phillips. 1981. Ion diffusion modified by tortuosity and volume fraction in the extracellular microenvironment of the rat cerebellum. *J. Physiol.* 321:225–257.

Nicholson, C., and E. Syková. 1998. Extracellular space structure revealed by diffusion analysis. *Trends Neurosci.* 21:207–215.

Nicholson, C., and L. Tao. 1993. Hindered diffusion of high molecular weight compounds in brain extracellular microenvironment measured with integrative optical imaging. *Biophys. J.* 65:2277–2290.

Noguchi, Y., J. Wu, R. Duncan, J. Strohalm, K. Ulbrich, T. Akaike, and H. Maeda. 1998. Early phase tumor accumulation of macromolecules: a great difference in clearance rate between tumor and normal tissue. *Jpn. J. Cancer Res.* 89:307–314.

Ogston, A. G., and E. F. Woods. 1953. Molecular configuration of dextrans in aqueous solution. *Nature.* 171:221–222.

Pérez-Pinzón, M. A., L. Tao, and C. Nicholson. 1995. Extracellular potassium, volume fraction and tortuosity in rat hippocampal CA1, CA3 and cortical slices during ischemia. *J. Neurophysiol.* 74:565–573.

Pluen, A., P. A. Metti, R. K. Jain, and D. A. Berk. 1999. Diffusion of macromolecules in agarose gels: comparison of linear and globular configurations. *Biophys. J.* 77:542–552.

Rice, M. E., and C. Nicholson. 1991. Diffusion characteristics and extracellular volume fraction during normoxia and hypoxia in slices of rat neostriatum. *J. Neurophysiol.* 65:264–272.

Rice, M. E., Y. C. Okada, and C. Nicholson. 1993. Anisotropic and heterogeneous diffusion in the turtle cerebellum: implications for volume transmission. *J. Neurophysiol.* 70:2035–2044.

Rosen, A. S., and R. D. Andrew. 1990. Osmotic effects upon excitability in rat neocortical slices. *Neuroscience.* 38:579–590.

Rubinow, S. I. 1975. Introduction to Mathematical Biology. Wiley, New York.

Rusakov, D. A., and D. M. Kullmann. 1998. Geometric and viscous components of the tortuosity of the extracellular space in the brain. *Proc. Natl. Acad. Sci. U.S.A.* 95:8975–8980.

Šubr, V., J. Strohalm, T. Hirano, Y. Ito, and K. Ulbrich. 1997. Poly[*N*-2-hydroxypropyl)methacrylamide] conjugates of methotrexate: synthesis and in vitro drug release. *J. Controlled Release.* 49:123–132.

Syková, E. 1997. The extracellular space in the CNS: its regulation, volume and geometry in normal and pathological neuronal function. *Neuroscientist.* 3:28–41.

Tao, L. 1999. Effects of osmotic stress on dextran diffusion in rat neocortex studied with integrative optical imaging. *J. Neurophysiol.* 81: 2501–2507.

Tao, L., and C. Nicholson. 1995. The three-dimensional point spread functions of a microscope objective in image and object space. *J. Microsc.* 178:267–271.

Tao, L., and C. Nicholson. 1996. Diffusion of albumins in rat cortical slices and relevance to volume transmission. *Neuroscience.* 75:839–847.

Ulbrich, K., M. Pechar, J. Strohalm, V. Šubr, and B. Říhová. 1997. Synthesis of biodegradable polymers for controlled drug release. *Ann. N.Y. Acad. Sci.* 831:47–56.

Wright, A. K., and M. R. Thompson. 1975. Hydrodynamic structure of bovine serum albumin determined by transient electric birefringence. *Biophys. J.* 15:137–141.

Zoli, M., A. Jansson, E. Syková, L. F. Agnati, and K. Fuxe. 1999. Volume transmission in the CNS and its relevance for neuropsychopharmacology. *Trends Pharmacol. Sci.* 20:142–150.